

# On the Ni-H System

S. FOCARDI<sup>(1)</sup>, V. GABBANI<sup>(2)</sup>, V. MONTALBANO<sup>(2)</sup>,  
F. PIANTELLI<sup>(2)</sup> and S. VERONESI <sup>(2)</sup>

<sup>(1)</sup> *Dipartimento di Fisica, Università di Bologna e  
INFN sezione di Bologna, Bologna - Italy*  
<sup>(2)</sup> *Dipartimento di Fisica, Università di Siena e  
Centro IMO Siena - Italy*

## 1 Introduction

We shall present here a review of the most important results obtained in experiments with Ni and H performed in the last decade. Furthermore, we report the last and more interesting evidence on nuclear reactions occurring in this system.

In section 2 we exhibit the experimental setup and some examples of the cell we utilized. In the following sections we illustrate four main topics: hydrogen loading, energy production, ionizing radiation and element transmutations.

## 2 Experimental setup

A schematic view of the experimental setup is shown in Fig. 1. Continuous data acquisition (voltage and current supplied to the cell heater, pressure, temperatures) is performed by means of a PC equipped with a 12 bit National Instrument interface card utilizing a Labview software. The vacuum system consists in a rotary pump and a turbomolecular pump.

In our experiments we utilized two different types of cell. In the former (Fig. 2) the sample has a rod geometry, while in the latter (Fig. 3) the samples have a slab geometry. In Fig. 2 and in Fig. 3 are also shown types and positions of the temperature sensors.

The samples were Ni (99.5% purity) or Ni alloys. In the following, for the sake of simplicity, we present essentially the results relative to the Ni samples. For more details concerning the experimental setup and the cells see references [1] [2] [3].

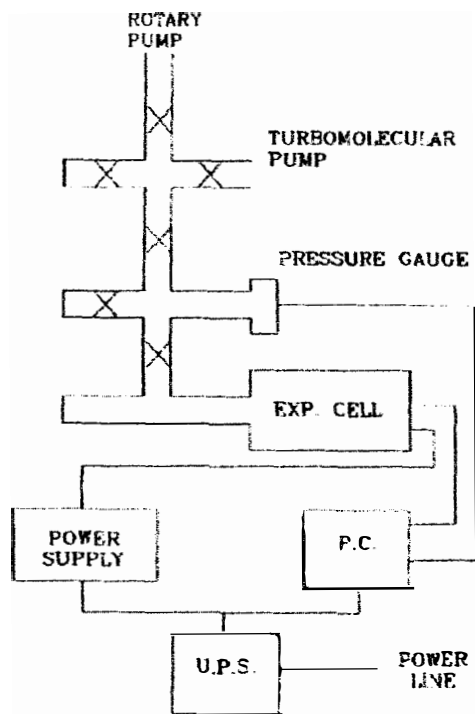


Figure 1: Experimental set-up.

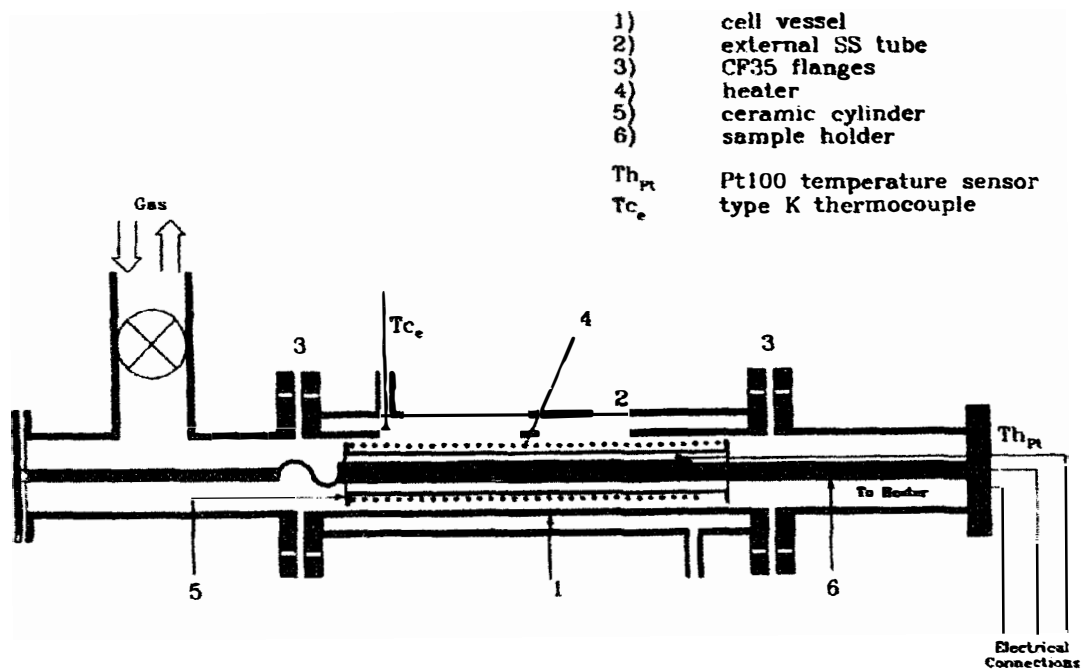


Figure 2: Schematic section of the cell for rod-like samples.

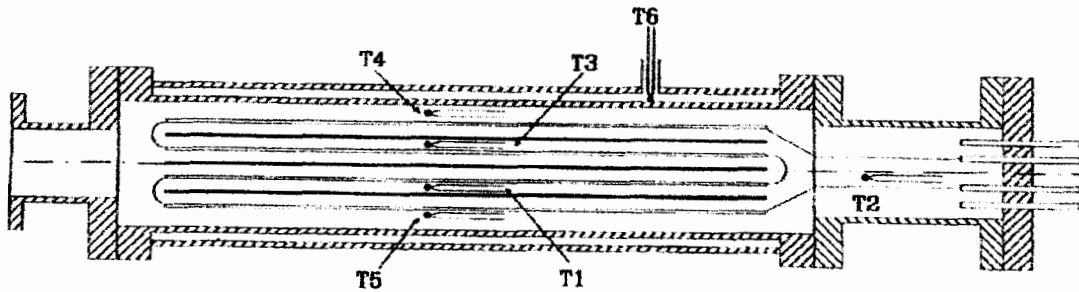


Figure 3: Schematic section of the cell for slab-like samples; T<sub>i</sub> shows the position of the thermocouples.

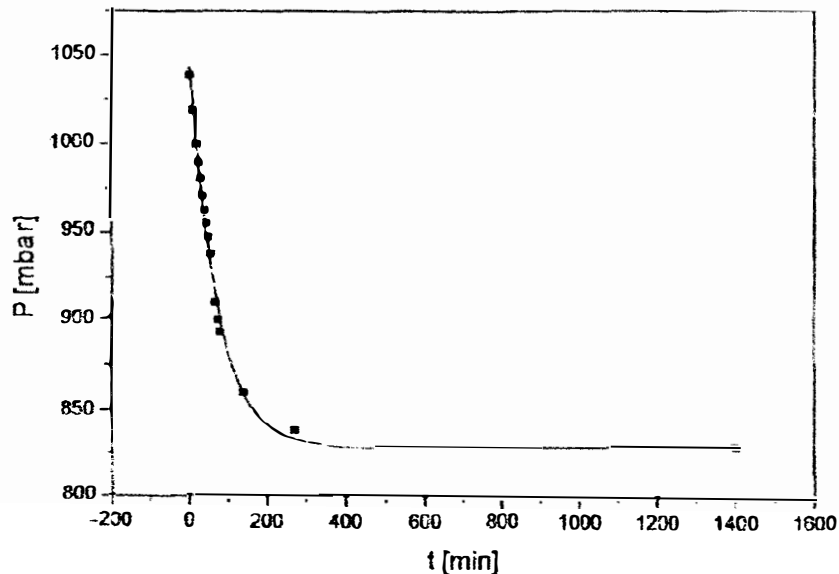


Figure 4: A typical hydrogen loading of a sample. The experimental data can be fitted with an exponential law. The characteristic time for this data set is  $\tau = 72$  minutes.

### 3 Hydrogen loading

The hydrogen loading in the nickel is done inside a closed vessel (the cell) kept at constant temperature (usually in the range 450-750 K) and at subatmospheric pressure (typically between .1 and 1 bar). Loading is measured by the pressure decreasing with time. In some cases one or more annealing cycles were performed previously. We are not able to estimate the importance of such preliminary operations.

The phenomenon appears to be strongly complex but shows many interesting features. A typical hydrogen loading is shown in Fig. 4. After a fast decreasing, the pressure goes asymptotically to an equilibrium value. Such a value depends on the sample history, as proved by the hysteresis cycle reported in Fig. 5. Furthermore, the loading rate changes with the equilibrium temperature as shown in Fig. 6.

One of the larger and faster loading we obtained, is shown in Fig. 7 [4]. In this case, the measured ratio between H and Ni is  $(5.9 \pm .8)10^{-3}$ , on assuming a bulk loading. Such an amount is about 70 times larger than the literature values [5] [6]. Similar

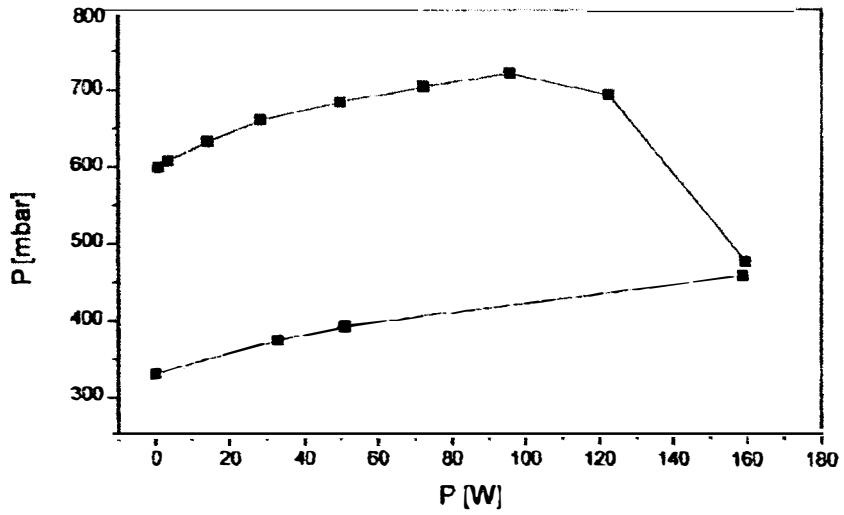


Figure 5: A pressure vs temperature plot. The cycle, showing a  $H_2$  absorption, was covered clockwise. Dots refer to equilibrium states.

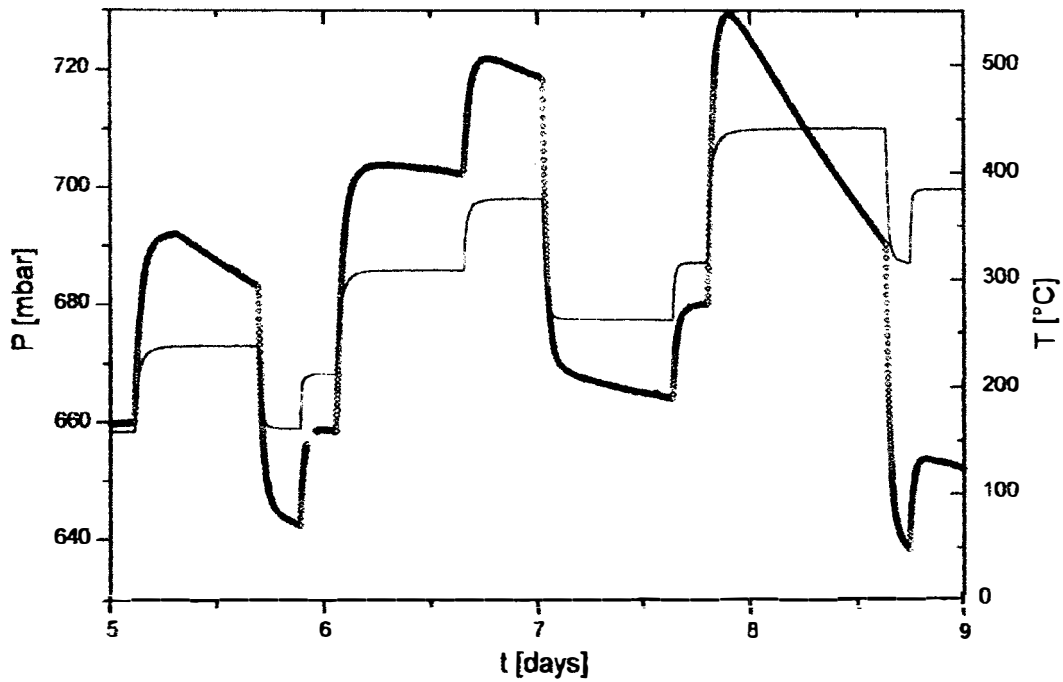


Figure 6: Pressure vs time (diamonds) and Ni temperature vs time (line). The two curves evidence the dependence of the hydrogen loading rate on the temperature.

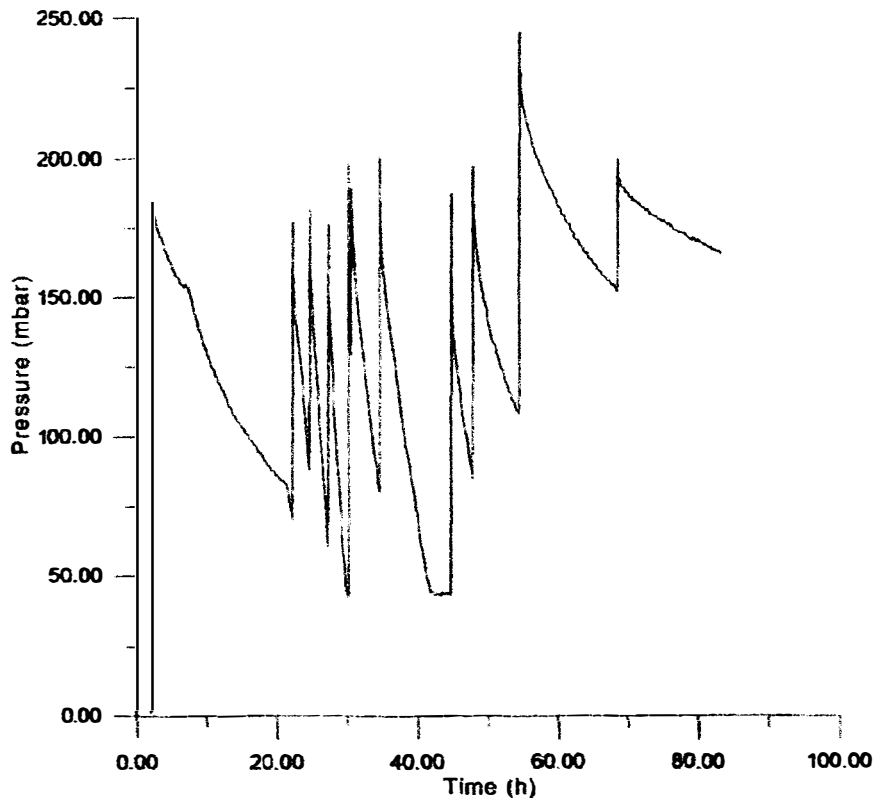


Figure 7: A pressure vs time plot at the same temperature showing a series of absorptions following hydrogen refilling.

discrepancies have been already remarked by other authors [7] who evidenced the dependence of the experimental results on the history of the samples. In fact, in some experiments we also obtained poor loading. Furthermore in rare cases the loading was not obtained.

## 4 Energy production

Our experimental cells can be described, from a thermodynamical point of view, as black boxes to which a heater supplies an electric power up to 150 W.

As is well known, at the thermal equilibrium, the temperatures of the external wall depend only on the power dissipated into the cell, from the thermal bath temperature and from the exchange coefficient between the wall and the thermal bath. This model is well verified if the internal hydrogen pressure is greater than 100 mbar, as in our usual working conditions.

The exchange coefficient can be considered as a constant in a small temperature range, as shown by the experimental data. In this way it is possible from the calibration curve ( $\Delta T$  versus power), to deduce the total power amount dissipated into the cell by measuring the temperature difference between the cell external wall and the thermal bath. Thus, an eventual power excess can be measured by the difference between the total power and the supplied power [1] [2].

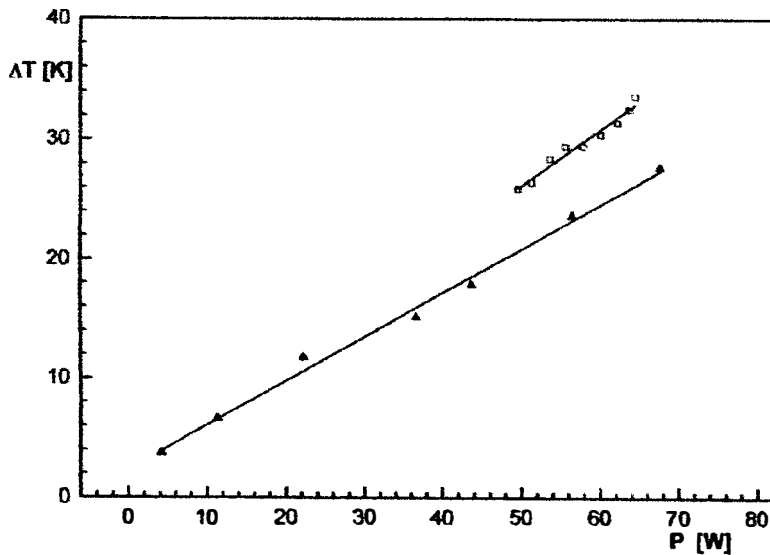


Figure 8 External wall temperature (relative to the room temperature) vs power. The lower curve is the calibration, while the upper points refer to a power production.

Fig. 8 shows both a typical calibration curve and another corresponding to an energy production. The comparison between the two curves allows us to estimate, in this case, a power excess of about 18 W.

The general method of bringing a cell from its normal state, described by the calibration curve, to an excited state (with energy production) consists in a perturbation of its thermodynamical parameters. Fig. 9 shows the time evolution of the temperatures of a cell during a transition to the excited state induced by a thermal jump.

The two cells which have produced energy for the longest time were active respectively for 278 and 319 days giving off 900 MJ and 600 MJ. By considering the amount of Ni and H involved, such quantity of energy cannot be explained by chemical processes.

We want to note here some important features of our system:

a) the possibility of changing the state of the cell from normal to excited and *vice versa*, after the first transition. This means that the process can be controlled.

b) the existence of several excited stationary states and their stability for long time periods

c) the existence of a threshold temperature (about 450 K for the Ni-H system) under which we were not able to obtain or to maintain the excited state

In our opinion, these features suggest a non-linear nature of the phenomenon which could be due to an anharmonic effect that dominates above the Debye temperature.

## 5 Ionizing radiation

The important feature that our system can be active for long time allowed us a systematic search for ionizing radiation coming from the cell. In fact long time monitoring allows one to put in evidence, because of a good statistics, also small intensity effects and to increase the probability to observe sporadic emissions which do not change the

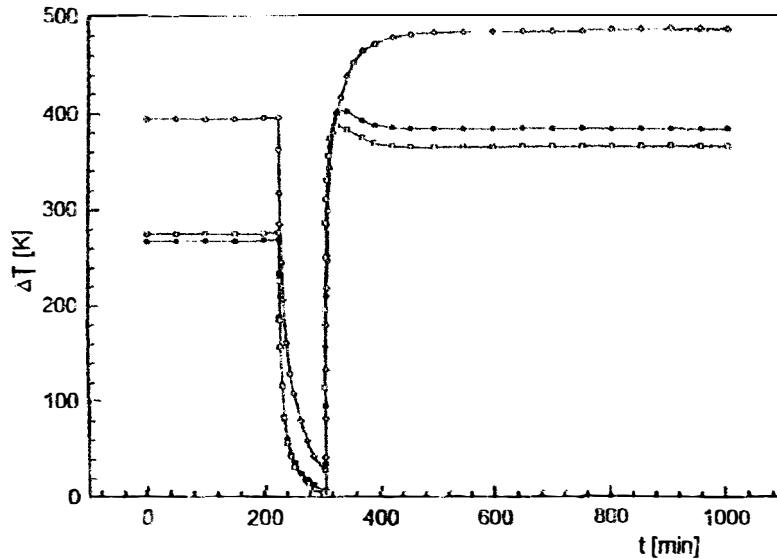


Figure 9: A sample excitation performed with a temperature jump ( $T_{c1}(\diamond)$ ,  $T_{c2}(\bullet)$ ,  $T_{c3}(\square)$  are the temperatures in the positions shown in Fig. 2). An inversion between  $T_{c2}$  and  $T_{c3}$  can be observed. Such an effect is due to the extra power produced by the nickel rod.

macroscopic stationary state. We report here the experimental evidence of neutrons and gamma rays emission.

## 5.1 Neutron measurements

We obtained a relatively strong neutron emission only in a short time period of about one month. Successively, in the same experiment [8] [9], we observed a smaller effect which lasted about three months. In the first period, characterized by a spontaneous increase of the cell power, the neutron flux was high enough to allow the activation of a gold sheet. The gold sheet was placed inside a paraffin box (for neutron thermalization) very close to the cell [9]. After some days the sheet was placed on a high purity germanium (HPGe) detector. Fig 10 shows the characteristic 411.8  $\gamma$ -rays peak coming from the  $Au^{198}$  decay process. By comparison with the effect produced by an Am-Be source of known strength, we evaluated an emission yield of about 6000 neutrons/s.

In the successive period an emission yield of  $\sim 2$ -5 neutrons/s only was measured [9].

## 5.2 Gamma-rays measurements

In the last experiments the setup was modified by adding  $\gamma$  detectors. In particular we used a NaI 4" x 4" detector and a HPGe detector monitoring the same cell.

In three successive experiments performed with the cell shown in fig. 3, we observed for some days an emission of  $\gamma$ -rays. Fig 11 which refers to the first (of the three) experiment shows the existence of three peaks above the background. Fig. 12 was obtained during the second experiment. From the analysis of the NaI spectra we established the following energies for the three peaks:  $E_1 = 650 \pm 40$  keV,  $E_2 = 1500 \pm 50$  keV,  $E_3 = 2600 \pm 60$  keV. Furthermore the HPGe detector allows one to obtain a better

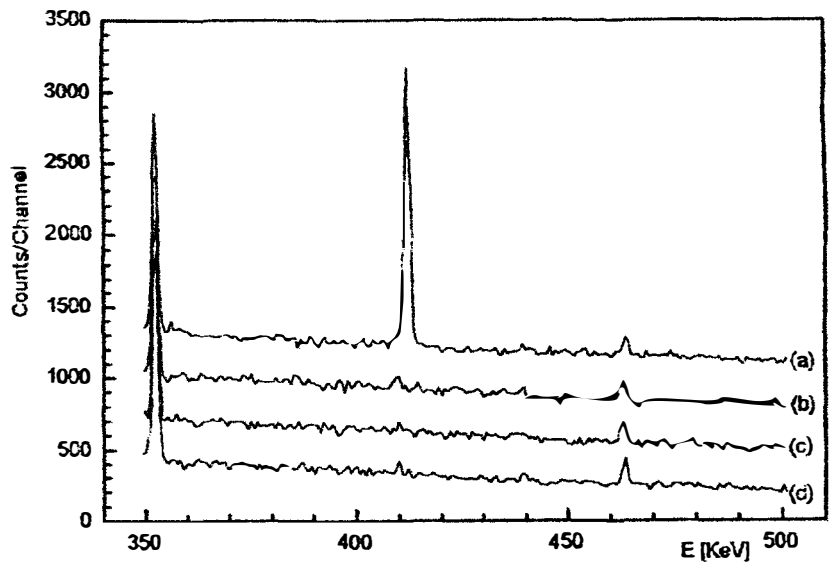


Figure 10: Gamma ray spectra in the 350-500 keV region obtained with a germanium detector for: (a) gold sheet after the activation for 12 days on the cell; (b) gold sheet after the same exposition time to cosmic rays 10 m away from the cell; (c) gold sheet before the activation on the cell; (d) laboratory background.

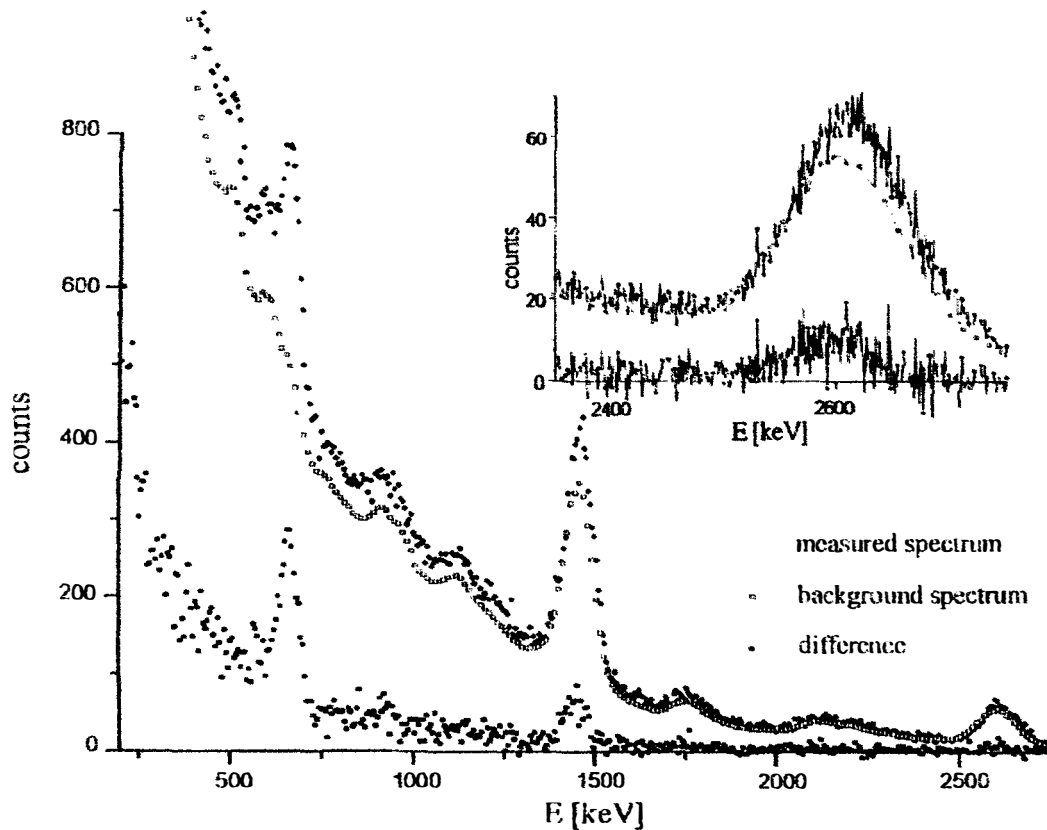


Figure 11: First experiment: background and measured spectra. The background spectrum is a mean of 90 acquisitions ("live" time 12000 s) while the measured one is a mean of 6 acquisitions. The lower curve is the difference between measured and background spectrum.



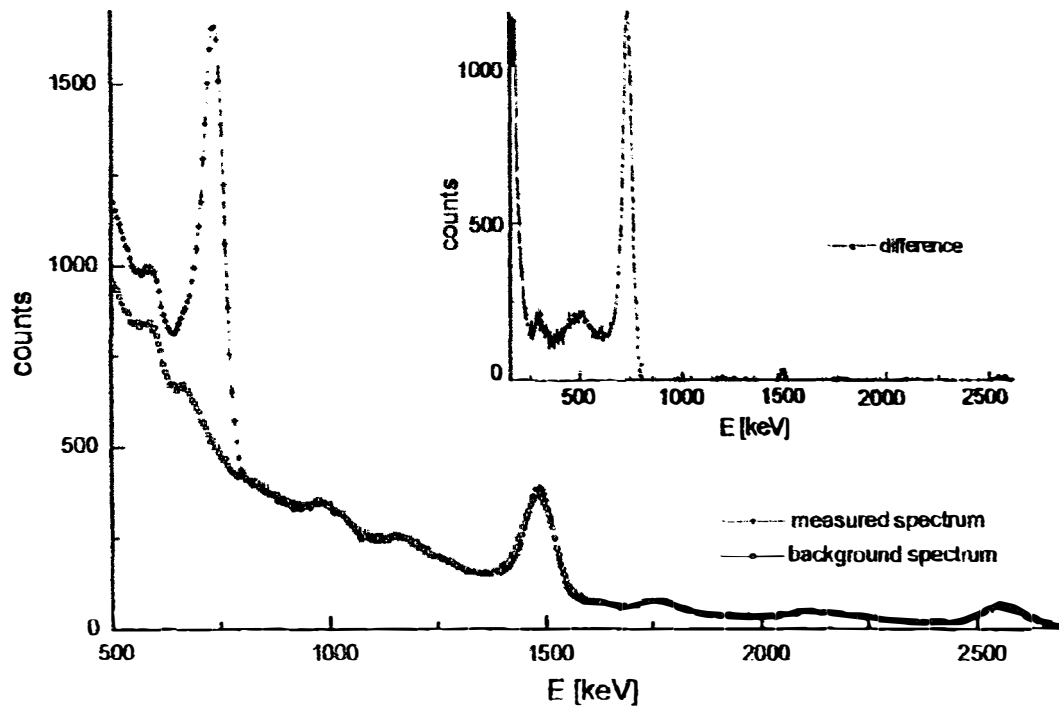


Figure 12: Second experiment: background and measured spectra. The background spectrum is a mean of 20 acquisitions ("live" time 18000 s) and the measured one is a mean of 30 acquisitions. The lower curve is the difference between measured and background spectrum.

measurement of the energy of the first peak:  $E_1 = 661 \pm 1$  keV.

The most important features of the  $\gamma$  radiation in these experiments are the following:

- a) the ratio between the peak intensity changes also in the same experiment during the time. This behaviour indicates that the  $\gamma$ -rays observed arise from different processes.
- b) The peaks were observed only for a narrow period (relative to the experiment length) of the order of a month [3].
- c) The intensities of the peaks change abruptly in a time much less than 12000 s (our data acquisition live time).

## 6 Element transmutations

At the end of each experiment we systematically analyzed the sample surfaces by using the scanning electron microscope (SEM) equipped with energy dispersive X-ray (EDX) system. These analyses are compared with those performed on nickel samples from the same batch and cleaned in the same way (reference samples).

The two EDX spectra shown in fig. 13 refer to different surface regions of the same sample. The first region (fig. 13a) remained unchanged during the treatment process in the cell, while the second one (fig. 13b) is characterized by strong morphological modifications. The presence in the second spectrum of several elements different from the nickel [12] is a further proof that nuclear processes occurred in the sample. Similar

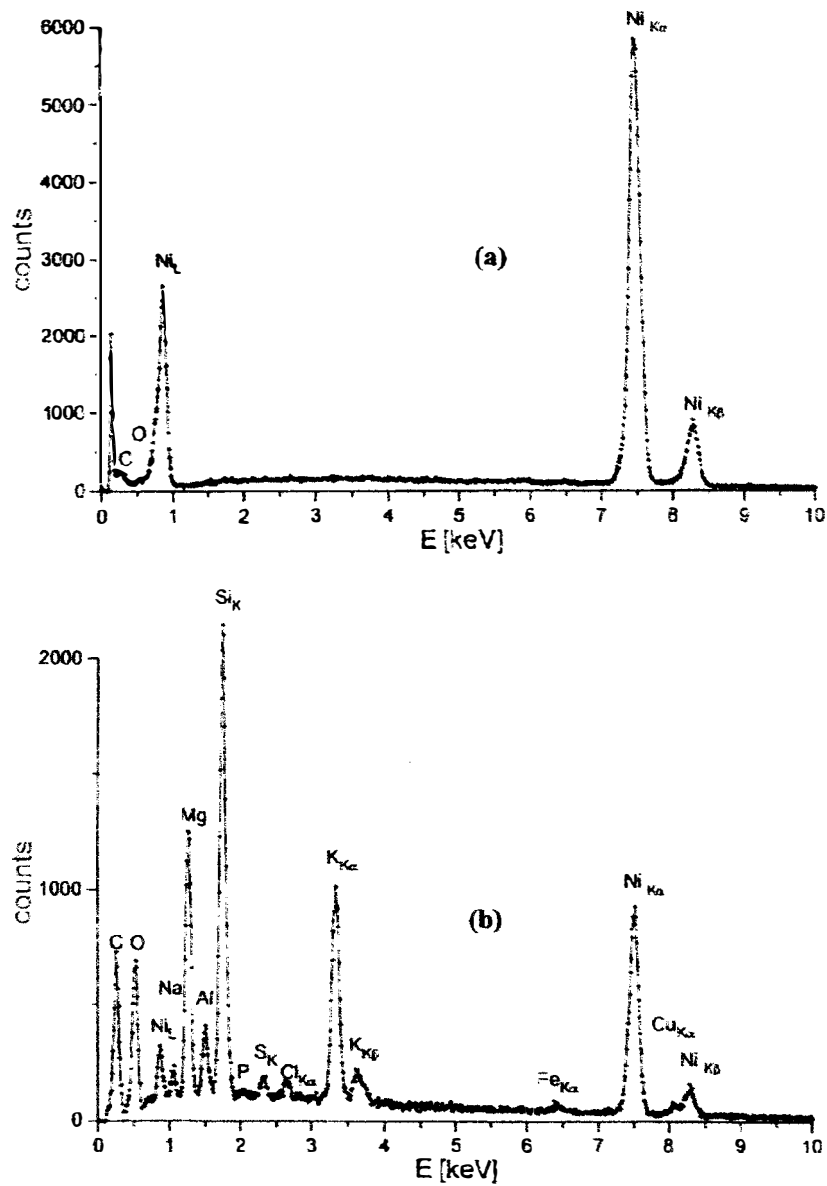


Figure 13: EDX spectra (number of X-rays emitted by fluorescence versus their energy) obtained with electrons accelerated to 25 keV and relative to the same sample. Spectra refer to (a) a unchanged zone and (b) a morphologically modified region.

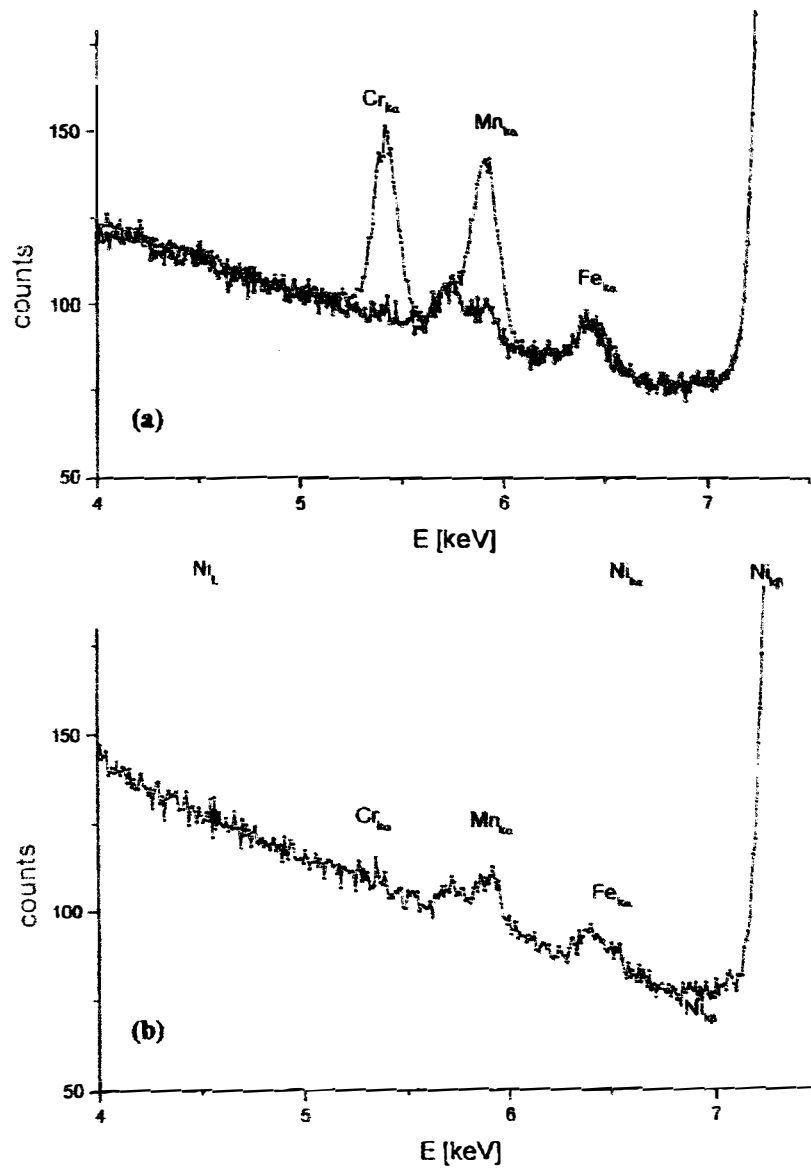


Figure 14: EDX spectra obtained with electrons accelerated at 25 keV relative to (a) a reference sample, (b) a sample from the first experience, (c) a sample from the second experience.

results were been obtained, in electrolytic experiments, by other authors [13] [14].

The first two experiments in which  $\gamma$  emission was detected had different behaviour regarding the energy production. In fact in the first experiment there was a macroscopic power production ( $P \sim 20$  W), which did not occur in the second one. Fig. 14 shows the EDX spectra obtained from a reference sample and from the samples treated in these two experiments. The two samples remained into the same cell in the same thermodynamic conditions and were prepared in the same manner. Moreover, the second one was kept into the cell for a longer time (almost twice the first one). Thus we can conclude that the presence of Cr and Mn could be strictly related to the power production and not a consequence of contaminations.

## 7 Conclusions

Our experiments proof without any doubt that

a) the hydrogen loading into the nickel is much greater than the literature values, under our working conditions.

b) the Ni-H system can produce an amount of energy not explainable with chemical processes,

c) the power production can be switched on or off in a controlled way,

d) nuclear reactions occur in the system.

Finally we want to underline that we do not have any interpretation on the nuclear chains occurring in our samples. Work is in progress to increase the experimental data in order to identify the main of such chains.

## Acknowledgments

We are grateful to the current and the past director of the Siena physics department A. Scribano and L. Moi for their support. We wish to thank profs. P.G. Bergamini, L. Daddi and P.G. Sona for helpful suggestions and discussions. The technical support of C. Stanghini was crucial for the realization of the experimental apparatus.

## References

- [1] S. Focardi, R. Habel and F. Piantelli, *Nuovo Cim. A*, 107 (1994) 163.
- [2] S. Focardi, V. Gabbani, V. Montalbano, F. Piantelli and S. Veronesi, submitted to *Nuovo Cim. A*.
- [3] S. Focardi, V. Gabbani, V. Montalbano, F. Piantelli and S. Veronesi, to be published.
- [4] A. Ventura, thesis, Bologna University, 1996.
- [5] Y. Fukai, *The metal-hydrogen system*, Springer-Verlag (1993)
- [6] C.J. Smithells, *Metals reference book*, pag. 535, Butterworths Scientific Publications, (1955).

- [7] L.H. Germer, A.V. MacRae and C.D. Hartman, *Jour. of Appl. Phys.*, 32, (1961) 2432.
- [8] S. Focardi, V. Gabbani, R. Habel, V. Montalbano, F. Piantelli, G. Salvetti, E. Tombari and S. Veronesi, *Status of cold fusion in Italy, IV - Proceedings of Siena workshop, Siena, 24-25 March 1995, to be edited by B. Stella.*
- [9] A. Battaglia, L. Daddi, S. Focardi, V. Gabbani, V. Montalbano, F. Piantelli, P.G. Sona and S. Veronesi, submitted to *Nuovo Cim. A.*
- [10] A.B. Garg, R.K. Rout, M. Srinisavan, T.K. Sankarnarayanan, A. Shyam, and L.V. Kulkarni, *Proceedings of the ICCF-5, Monte-Carlo, Monaco 9-13 April (1995) and references therein.*
- [11] A. Shyam, M. Srinisavan, T.C. Kaushik, and L.V. Kulkarni, *Proceedings of the ICCF-5, Monte-Carlo, Monaco 9-13 April (1995) and references therein.*
- [12] S. Focardi, V. Gabbani, V. Montalbano, F. Piantelli and S. Veronesi, *Atti Accad. Fisiocritici, Serie XV, Tomo XV, (1996) pgs. 109-115.*
- [13] G.H. Miley and J. A. Patterson, *Infinite Energy*, 19, July-August 1996.
- [14] T. Ohmori and M. Enyo, *Jour. New Energy*, 1, 1, (1996) 15.